Available online at www.sciencedirect.com
ScienceDirect
Catalysis Today 133–135 (2008) 565–573
CATALYSIS TODAY
www.elsevier.com/locate/cattod

# Hydrogen production from biomass-derived oil over monolithic Pt- and Rh-based catalysts using steam reforming and sequential cracking processes

Marcelo Eduardo Domine, Eduard Emil Iojoiu, Thomas Davidian, Nolven Guilhaume *, Claude Mirodatos

*Institut de Recherches sur la Catalyse et l'Environnement de Lyon, UMR 5256 CNRS-Université Lyon 1, 2 Avenue Albert Einstein, F-69626 Villeurbanne Cedex, France*

Available online 28 January 2008

**Abstract**

The conversion of biomass-derived crude oil towards $H_2$ production was investigated using continuous catalytic steam reforming and sequential cracking/reforming processes. The performances of $Pt/Ce_{0.5}Zr_{0.5}O_2$ and $Rh/Ce_{0.5}Zr_{0.5}O_2$ catalysts deposited on cordierite monoliths were comparatively studied. The Pt-based catalyst showed better catalytic activity than Rh for steam reforming in the whole range of steam-to-carbon molar ratios (S/C) studied, the amount of added water determining the $H_2$ yield for both noble metals. The best $H_2$ yield (70%, corresponding to ~49 mmol of $H_2$/g of bio-oil) was obtained with the Pt catalyst at S/C ratio of 10 at 780 °C, with $CH_4$ concentrations below 1%. In the case of sequential cracking, the process alternated cracking steps, during which the bio-oil is converted into $H_2$, CO, $CO_2$, $CH_4$ and carbon stored on the catalyst, with regeneration steps where the deposited coke was burnt under $O_2$. Comparison with thermal bio-oil cracking showed that the catalyst plays a major role in enhancing the $H_2$ productivity up to 18 mmol of $H_2$/g of bio-oil (~50% of $H_2$ in gaseous products stream) and lowering the $CH_4$ formation. The steam reforming offers high yields towards $H_2$ but is highly endothermic, whereas the sequential cracking, despite lower $H_2$ yields, offers a better control of coke formation and catalyst stability, and due to lower energy input can theoretically run auto-thermally.


*Keywords:* Hydrogen production; Biomass valorization; Pyrolysis bio-oil; Catalytic steam reforming; Noble metal; Ceria–zirconia; Monolith

## 1. Introduction

The main existing process for hydrogen production is catalytic steam reforming of natural gas and oil-derived naphtha. Partial oxidation of heavy oil residues and coal gasification are also applied at industrial level, although less widespread. All these processes utilize fossil resources and produce $CO_2$ that contributes to the greenhouse effect. Alternatively, hydrogen might be generated starting from renewable sources, such as biomass. However, to avoid utilizing subsistence crops such as vegetable oils [1] or sugars [2], renewable lignocellulosic biomass could be used as alternative feedstock for hydrogen production. Two possible routes have been studied for lignocellulosic biomass treatment: direct steam gasification [3–5], or catalytic steam reforming of the bio-liquids derived from fast pyrolysis of biomass, commonly named bio-oils [6]. Since the production of bio-oils is now a mature technology [7], their catalytic treatment to produce hydrogen can be the most promising technology for a clean and renewable hydrogen generation. Fast pyrolysis liquids are complex mixtures of oxygenated compounds emulsified with water. They contain acids, aldehydes, ketones, alcohols, glycols, esters, ethers, phenols and derivatives, as well as carbohydrates, and a large proportion (20–30 wt.%) of lignin-derived oligomers [8]. The bio-oils could be treated directly as a whole or using specific fractions. Nevertheless, direct feeding of the entire bio-oil into the reformer reactor is not easy, since it is only partly soluble in water and highly unstable upon heating, polymerizing at temperatures as low as 80 °C.

Catalytic steam reforming of some oxygenated molecules, such as methanol, acetic acid, ethanol, acetone, phenol or

* Corresponding author. Tel.: +33 472 44 53 89; fax: +33 472 44 53 99.
*E-mail address:* Nolven.Guilhaume@ircelyon.univ-lyon1.fr (N. Guilhaume).

0920-5861/$ – see front matter © 2007 Elsevier B.V. All rights reserved.
doi:10.1016/j.cattod.2007.12.062

cresol, used as model compounds of bio-oils [9–14], has been investigated in the last decade. Ni supported on $Al_2O_3$, and mixtures of $Al_2O_3$ and other metal oxides (e.g. $La_2O_3$ or MgO), have been mainly used as catalysts in these processes [10–12]. Despite the fact that noble metals such as Ru or Rh are efficient in steam reforming reactions and limit coke formation compared to Ni, only few examples of their use have been mentioned until now [13,14]. Other previous works include the use of the water-soluble fraction (which contains carbohydrate-derived compounds) of bio-oil derived from poplar wood as feed for hydrogen production, through steam reforming process over Co- or Cr-promoted Ni/α-$Al_2O_3$ catalysts [15]. In this case, $H_2$ productivities close to 200 g of $H_2$/kg of catalyst/h can be reached.

Recently, Rioche et al. [16] have reported the successful use of model compounds as well as crude bio-oil as feedstock for catalytic steam reforming towards hydrogen production, by using noble metal-based catalysts supported on alumina or on ceria–zirconia materials. The latter support leads to higher $H_2$ yields compared to alumina-supported catalyst. In a recent study, our research group has proved the good activity and stability of Ni–K/$La_2O_3$–$Al_2O_3$ catalyst in a sequential cracking/reforming reaction using crude bio-oil as feed [17]. The process alternates cracking steps, during which a $H_2$ + CO-rich stream is produced and carbon is stored on the catalyst, with regeneration steps where the carbon is combusted under oxygen. With this process, the cracking steps yielded 45–50% of $H_2$ in the products stream.

Herein, we report the study of steam reforming reactions for hydrogen production over Pt- and Rh-supported on ceria–zirconia materials, by using the whole bio-oil as feedstock, and not only the aqueous fraction as commonly reported in the literature. The catalysts were tested supported onto a cordierite monolith in order to limit the pressure drop expected from fixed-bed reactors with powdered catalysts. The continuous steam reforming process and the two-step cracking/regeneration alternative process (namely sequential cracking process) are compared in terms of catalytic performances, $H_2$ production, technical feasibilities and energetic aspects.

## 2. Experimental

### 2.1. Bio-oil

The crude bio-oil sample was produced by BTG and supplied by the University of Twente. It was produced by fast pyrolysis of beech wood residues in the absence of $O_2$ (temperature around 500 °C, time of residence <1 s). It appears as a dark brown liquid with a strong smoky odor, its viscosity at 20 °C is 45.1 cSt and its pH = 3.3. The bio-oil is a complex mixture of 200–300 compounds, essentially composed of oxygenated hydrocarbons, water (28.8 wt.%) and probably traces of metals like K, Mg, Ca (not analyzed). The elemental analysis data (C: 38.70; O: 53.40; H: 7.50; N: 0.38; Cl: 0.02; S: 0.08%) correspond to the average composition $CH_{1.32}O_{0.54}$ calculated on a dry basis, or $CH_{2.3}O_{1.04}$ including the water. The bio-oil was supplied filtered to remove char particles and was used for the catalytic tests without any pre-treatment.

### 2.2. Catalysts

The Pt/$Ce_{0.5}Zr_{0.5}O_2$ and Rh/$Ce_{0.5}Zr_{0.5}O_2$ catalysts were provided by Johnson Matthey as powders or coated on a cordierite monolith (20 mm diameter, 17 mm length, 1200 cpsi). The average weight of coated monoliths was around 2 g. The metal loading and the specific surface area of used catalytic samples are summarized in Table 1.

Specific surface areas were calculated from the nitrogen adsorption isotherms at −196 °C (77 K), using a multipoint method. In the case of monoliths, a specially designed cell was used to measure the surface area avoiding the monolith destruction. Chemical analyses of catalysts were performed before and after reactions.

### 2.3. Reaction setup and product analysis

Bio-oils cannot be vaporized before feeding into the reactor, since they polymerize at 80 °C and decompose upon heating, while the reforming reactor must be operated at temperatures higher than 650 °C to be efficient. For this reason, a double envelope stainless steel tubular reactor equipped with water-cooling was designed to inject the cooled bio-oil (below 50 °C) through a capillary on top of the hot catalyst (fixed-bed) by working in down-stream regime. The bio-oil was sent with a syringe pump, at flow rates in the 1–5 mL/h range. In the case of continuous steam reforming tests, the reactor was equipped with a second capillary injector connected to a syringe pump for water introduction. For sequential cracking tests, an automated two-position switching valve sent the bio-oil either in the reactor, or in a collector tank. In order to restrict the heated zone to the catalyst bed, the oven consisted in a high-temperature heating tape winded tightly around the reactor. The system was also equipped with a pressure sensor and a thermocouple placed inside the catalyst bed. Water and other condensable products were trapped in an ice-cooled condenser at the reactor outlet, allowing integral evaluation of water production/consumption over a given period on stream.

Table 1
Physical and textural properties of noble metals/ceria–zirconia washcoated on cordierite monoliths

| Catalyst | Noble metal[a](wt.%) | Surface area[a] ($m^2$/g) | Washcoat (wt.%) |
|---|---|---|---|
| Pt/$Ce_{0.5}Zr_{0.5}O_2$ on monolith | 1.00 | 118 | 13.9 |
| Rh/$Ce_{0.5}Zr_{0.5}O_2$ on monolith | 1.04 | 125 | 16.5 |

[a] Referred to the washcoat only (not including the cordierite mass).

The gaseous products obtained during the reactions were analyzed with two HP6890 GC in series, equipped with FID and TCD detectors. Three capillary columns allowed the quantitative analysis of oxygenated compounds (alcohols, acids, aldehydes, ketones, compounds up to $C_{20}$), $C_1$–$C_5$ hydrocarbons, and permanent gases ($H_2$, CO, $CO_2$, $CH_4$). A mass spectrometer (VG-Prolab) with a closed ion source was used to follow transient experiments and permanent gases quantification. For water analysis, only few amounts were detected by mass spectrometry during the reaction process (steam reforming or sequential cracking/reforming processes), practically all the water present in the outlet gaseous mixture was trapped in the condenser placed before MS and GC analysis system. Then, the mean concentration of water was quantified by weighting the amount collected in the cold trap during the reaction process, including regeneration step (or the overall reaction cycle: cracking/purge/regeneration in the case of sequential cracking process).

The gaseous products stream was continuously and quantitatively analysed by mass spectrometry (MS) during the steam reforming and sequential cracking experiments. In addition, gas chromatography (GC) analyses were performed every 20 min, and the compositions were calculated on a dry basis, i.e., without water and diluent free (argon).

The carbon balance was calculated by comparing the total amount of carbon obtained from all the gaseous carbon containing compounds (CO, $CO_2$, $CH_4$, $C_2$+) formed during the bio-oil conversion (steam reforming or cracking/regeneration steps for the case of sequential process, including traces of organics dissolved in the water trap at the reactor outlet, and few amounts of carbon soot deposited at the bottom of the reactor), to the amount of carbon introduced in the bio-oil feed during the reaction process. The oxygen and hydrogen balances were evaluated as well, by comparing the total amount of O and H obtained from the O and H containing compounds ($H_2O$, CO, $CO_2$, $CH_4$, $C_2$+) formed along the bio-oil conversion, to the amount of H and O introduced in the bio-oil feed during the process. Weighing the water collected in the cold trap at the reactor outlet allowed semi-quantitative evaluation of the amount of unreacted water. In all cases these balances were found to be within the acceptable range 90–100%.

The $H_2$ productivity (Eq. (1)) was calculated as the quantity of $H_2$ produced (in mmol) per unit of bio-oil introduced (g). In the case of continuous steam reforming tests, the $H_2$ yield (Eq. (2)) was calculated as the ratio between the $H_2$ produced and the theoretical quantity of $H_2$ obtained when the complete reforming takes place.

$$H_2\ \text{prod.} = \frac{\text{mmoles of } H_2 \text{ produced}}{\text{g of bio-oil feeding}} \quad (1)$$

$$H_2\ \text{yield}\ (\%) = \frac{\text{moles of } H_2 \text{ obtained}}{2.12 \times \text{moles of carbon feeding}} \times 100 \quad (2)$$

### 2.4. Catalytic experiments

Typically, 2 g of monolith catalysts were introduced into the fixed-bed tubular reactor system described in the previous section. The catalysts were reduced under hydrogen at 350 °C (30 vol.% of $H_2$ in Ar, total flow 100 mL/min) prior to catalytic activity measurements.

#### 2.4.1. Steam reforming tests

The steam reforming experiments were carried out over monolithic catalysts at 700 and 780 °C under different steam-to-carbon molar ratios (S/C = 2.5, 5 and 10). These different S/C ratios were obtained by varying the bio-oil flow in the 1.2 and 5 mL/h range, whereas the water flow was maintained at 9 mL/h. When the same catalyst was tested successively at different S/C molar ratios, a regeneration step (carbon combustion at the reaction temperature in 20 vol.% of $O_2$ in Ar, total flow = 100 mL/min, followed by a pre-activation step under argon flow) was done after each experiment in order to ensure a standardized initial state.

#### 2.4.2. Sequential cracking tests

In a standard experiment, the catalyst was heated at 700 °C under a flow of 100 mL/min Ar. The sequential cracking tests were carried out by alternating a cracking step, during which a bio-oil flow of 5 mL/h (diluted in a 100 mL/min Ar) is injected during 5 min, with a 10 min regeneration step during which the carbon deposited on the catalyst is burnt under a flow of 20 vol.% $O_2$ in Ar (total flow rate = 100 mL/min). These two steps were separated by a purge under 100 mL/min of Ar. The catalytic stability was evaluated over more than 30 sequences. More detailed descriptions of catalytic sequential cracking experiments are given in Refs. [17,18].

## 3. Results and discussion

If one considers a generic oxygenated molecule, the steam reforming reaction proceeds according to the following equation:

$$C_nH_mO_k + (n-k)H_2O \rightarrow nCO + (n+m/2-k)H_2 \quad (3)$$

in parallel with the water-gas shift equilibrium (Eq. (4)).

$$nCO + nH_2O \leftrightarrows nCO_2 + nH_2 \quad (4)$$

The overall process can be represented as follows:

$$C_nH_mO_k + (2n-k)H_2O \rightarrow nCO_2 + (2n+m/2-k)H_2 \quad (5)$$

In the case of the bio-oil used here (average composition $CH_{1.32}O_{0.54}$), by application of Eq. (5) the stoichiometry for the steam reforming reaction is defined as follows:

$$CH_{1.32}O_{0.54} + 1.46H_2O \rightarrow CO_2 + 2.12H_2 \quad (6)$$

Moreover, the thermal decomposition (Eq. (7)) has also to be considered for most of the oxygenated organic compounds.

$$C_nH_mO_k \rightarrow C_xH_yO_z + \text{carbon} + \textit{gases}\,(H_2, CO, CO_2, CH_4, \ldots C_xH_{x+2}) \quad (7)$$

In this case, the carbon is essentially a soot-like deposit as shown in Ref. [17].

Thus, assuming that after an initial partial decomposition of oxygenates different $C_xH_y$ species can be generated, they can consecutively be either reformed catalytically into syngas following equations reported above (Eqs. (3) and (4)), or cracked following the typical reaction described in Eq. (8).

$$C_xH_{2x+2} \rightarrow xC + (x+1)H_2 \quad \text{[cracking]} \tag{8}$$

Carbon formation responsible for catalyst deactivation occurs onto the surface during the process. As a consequence, the catalyst surface must be regenerated by oxidation of the carbon as shown in Eq. (9). The reforming/cracking process can be very selective depending on the adequate selection of support and active metal catalyst.

$$C + O_2 \rightarrow CO_2 \quad \text{[regeneration]} \tag{9}$$

### 3.1. Steam reforming of crude bio-oil over Pt and Rh monolithic catalysts

$Pt/Ce_{0.5}Zr_{0.5}O_2$ and $Rh/Ce_{0.5}Zr_{0.5}O_2$ catalysts supported on cordierite monolith were tested in the steam reforming of bio-oil. The influence of steam-to-carbon (S/C) ratio and reaction temperature on the catalytic behaviour was studied. Over the whole investigated range of steam-to-carbon ratio and temperature, the bio-oil was totally converted, the main products being $H_2$, $CH_4$, CO and $CO_2$ (>99.5% of the total gas production), with only traces of ethane, ethylene and benzene as by-products. However, the gas composition was calculated on dry basis taking into account only the four main gaseous products ($H_2$, $CH_4$, CO and $CO_2$).

Fig. 1 depicts the outlet gas products composition monitored by mass spectrometry at 780 °C and S/C = 10, over $Pt/Ce_{0.5}Zr_{0.5}O_2$ (a) and $Rh/Ce_{0.5}Zr_{0.5}O_2$ (b), respectively. The fluctuations observed in the outlet gas composition reflect changes in the bio-oil–water mixture composition at the reactor inlet. As a matter of fact, since the bio-oil and water flows are different in the two injection capillaries (Section 2), the overall composition of the resulting droplets might vary from each other. Moreover, the low liquid flow rates used in our experiments at laboratory scale are difficult to manage compared to pilot scale flows. Despite these fluctuations, the mean hydrogen production was found practically constant for both catalysts. With the $Pt/Ce_{0.5}Zr_{0.5}O_2$ catalyst (Fig. 1a), the hydrogen yield reached 70% whereas it was lower (52%) in the case of $Rh/Ce_{0.5}Zr_{0.5}O_2$ catalyst (Fig. 1b and Table 2).

#### 3.1.1. Comparison of performances of Pt- and Rh-based systems

The most significant results concerning the steam reforming of bio-oil over Pt/and $Rh/Ce_{0.5}Zr_{0.5}O_2$ supported on monoliths are summarised in Table 2. For comparison, additional data obtained from similar Pt catalyst operated under close operating conditions [16] are also given.

With the Pt-based catalyst, the hydrogen concentration increased from 59% to 71% at 700 °C (Table 2) when increasing the S/C molar ratio, whereas the methane concentration decreased under 1%. In the same time, the

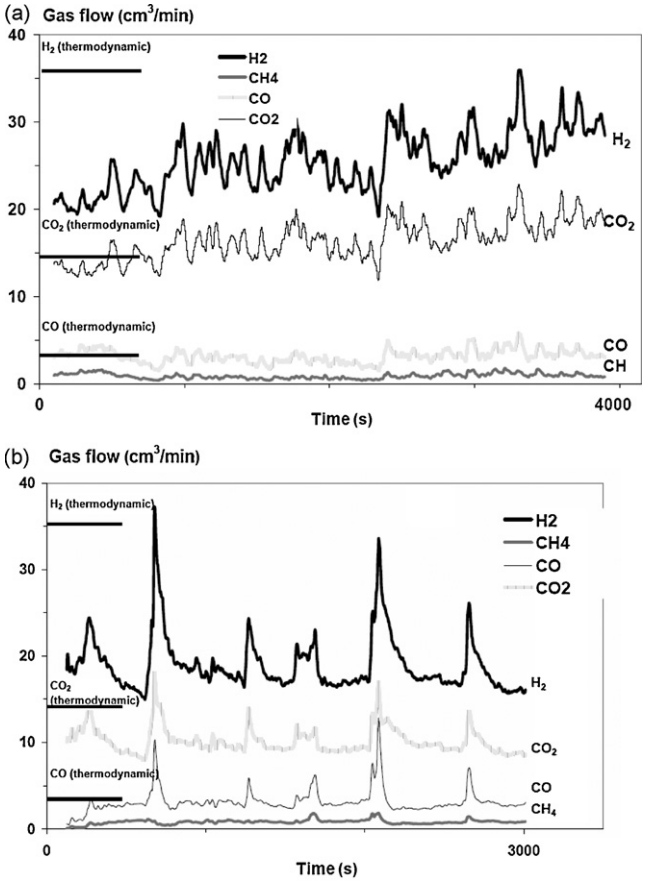


Fig. 1. Steam reforming of bio-oil over $Pt/Ce_{0.5}Zr_{0.5}O_2$ (a) and $Rh/Ce_{0.5}Zr_{0.5}O_2$ (b) on monolith catalyst at 780 °C and steam-to-carbon (S/C) molar ratio = 10. Reaction conditions: 9 mL $h^{-1}$ $H_2O$ flow, 1.2 mL $h^{-1}$ bio-oil flow, gas flow rate (Ar) = 100 mL $min^{-1}$. Products gas flows (mL $min^{-1}$) as monitored by mass spectrometer.

$CO_2$/CO ratio was found to increase (from 20/16 to 30/6) when the S/C molar ratio increases from 2.5 to 10. At 780 °C, the hydrogen concentration also changed from 62% to 67% by varying the S/C molar ratios from 2.5 to 10, while the $CH_4$ concentration fell again below 1% (Table 2). Increasing the temperature from 700 to 780 °C at S/C = 2.5 did not change much the hydrogen concentration: similar $H_2$ yields (30%) were obtained. At high S/C ratio, however, the hydrogen productivity and yield are clearly improved at the highest temperature. In the case of the $Rh/Ce_{0.5}Zr_{0.5}O_2$ catalyst supported on monolith (Table 2), the steam-to-carbon molar ratio was found to be the main factor that affects the outlet gas composition, the effect of temperature being only limited. By increasing the S/C molar ratio, both the $H_2$ concentration and the $CO_2$/CO ratio increase, as for Pt system. The best hydrogen yield (52%) was obtained at S/C = 10 and 780 °C.

Thus, for both catalytic systems, the conversion of bio-oil being complete at any conditions, increasing the S/C ratio clearly favours the production of $H_2$ and $CO_2$, as expected from a displacement of the WGS equilibrium, and enhances the secondary reforming of $CH_4$ produced by thermal decomposition.

Figs. 2 and 3 illustrate in more details the above-mentioned results, also including data obtained at S/C = 0.5 (no water

Table 2
Bio-oil steam reforming and sequential cracking experiments over noble metal catalysts supported on cordierite monolith

| | S/C ratio | Temperature (°C) | Gas composition (%) (calculated on dry basis) | | | | $H_2$ productivity (mmol/$g_{bio-oil}$) | $H_2$ yield (%) |
|---|---|---|---|---|---|---|---|---|
| | | | $H_2$ | $CH_4$ | CO | $CO_2$ | | |
| Steam reforming | | | | | | | | |
| $Pt/Ce_{0.5}Zr_{0.5}O_2$ | 2.5 | 700 | 59 | 5 | 16 | 20 | 21 | 30 |
| | | 780 | 62 | 2 | 6 | 30 | 21 | 30 |
| | 10.0 | 700 | 71 | <1 | 3 | 25 | 39 | 58 |
| | | 780 | 67 | <1 | 6 | 26 | 49 | 70 |
| $Rh/Ce_{0.5}Zr_{0.5}O_2$ | 2.5 | 700 | 52 | 9 | 25 | 14 | 21 | 30 |
| | | 780 | 56 | 6 | 23 | 15 | 22 | 33 |
| | 10.0 | 700 | 66 | 1 | 10 | 23 | 32 | 46 |
| | | 780 | 65 | 2 | 11 | 22 | 36 | 52 |
| Literature report [16][a] | 10.8 | 795 | 62 | 2 | 7 | 29 | – | 40 |
| | | | 66 | 1 | 9 | 24 | – | 65 |
| Sequential cracking[b] | | | | | | | | |
| $Pt/Ce_{0.5}Zr_{0.5}O_2$ | 0.5 | 700 | 49 | 7 | 30 | 15 | 17 | 45 |
| $Rh/Ce_{0.5}Zr_{0.5}O_2$ | 0.5 | 700 | 52 | 6 | 28 | 14 | 18 | 48 |
| Thermal decomposition[c] | 0.5 | 700 | 43 | 11 | 26 | 20 | 10 | 26 |
| Thermodynamic data[b] | 0.5 | 700 | 55 | 5 | 31 | 9 | >20 | >53 |

[a] Experimental conditions: 200 mg of 1 wt.%$Pt/Ce_{0.5}Zr_{0.5}O_2$ powder catalyst + 1000 mg cordierite; bio-oil flow = 0.84 mL/h; $H_2O$ flow = 5.8 mL/h; S/C = 10.8; $N_2$ flow = 50 mL/min.
[b] Sequential cracking/reforming experiments at 700 °C (no water addition). For more details see Ref. [18].
[c] Thermal cracking/decomposition experiment without catalyst (blank experiment).

added to the bio-oil, which will be discussed later) and 5, at 700 and 780 °C, respectively. For comparison, the thermodynamic equilibrium compositions for bio-oil steam reforming were also calculated at different temperatures, assuming a simplified bio-oil composition based on literature reports [8,18]: the relative concentrations of oxygenated components in the mixture (18 of the main bio-oil components, including water) were adjusted to match the ratio C:H:O revealed by the elemental analysis of the

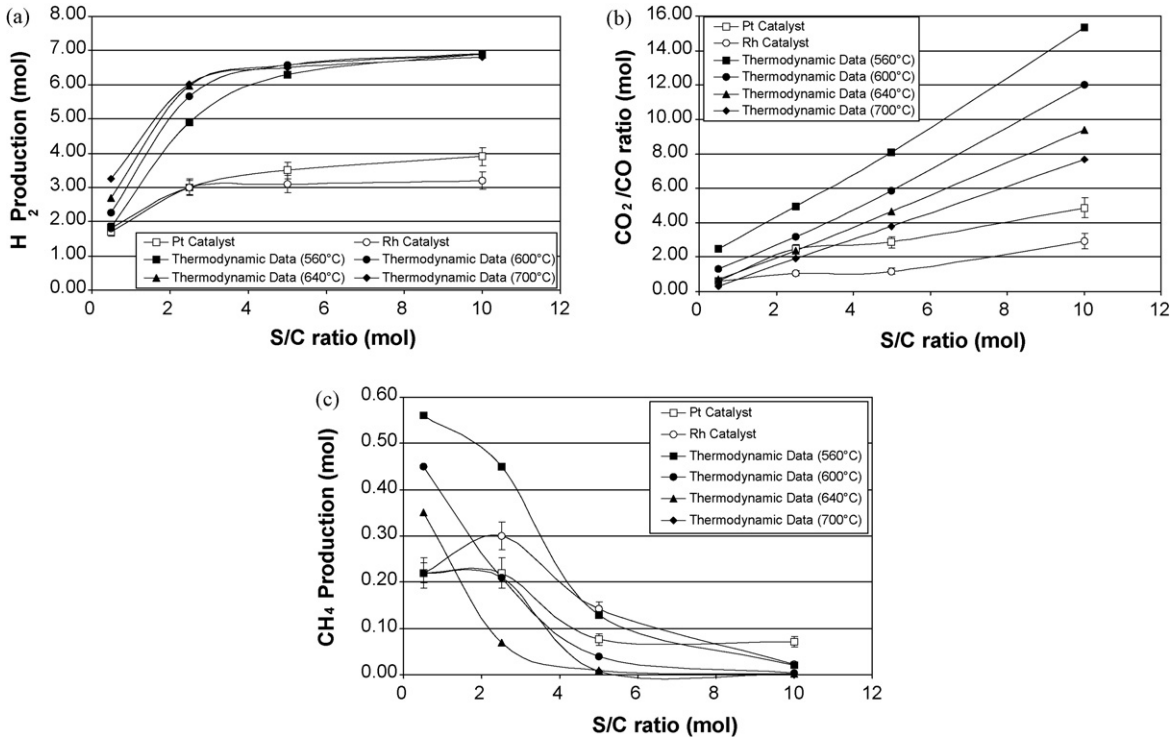


Fig. 2. $H_2$ production (a), $CO_2$/CO molar ratio (b) and $CH_4$ concentration (c) in function of the steam-to-carbon (S/C) molar ratios in the steam reforming of bio-oil over $Pt/Ce_{0.5}Zr_{0.5}O_2$ and $Rh/Ce_{0.5}Zr_{0.5}O_2$ on monolith catalysts at 700 °C. Comparison with thermodynamic data. Reaction conditions: 9 mL $h^{-1}$ $H_2O$ flow, 5, 2.5 and 1.2 mL $h^{-1}$ bio-oil flow, gas flow rate (Ar) = 100 mL $min^{-1}$. Data obtained from mass spectrometer analysis.

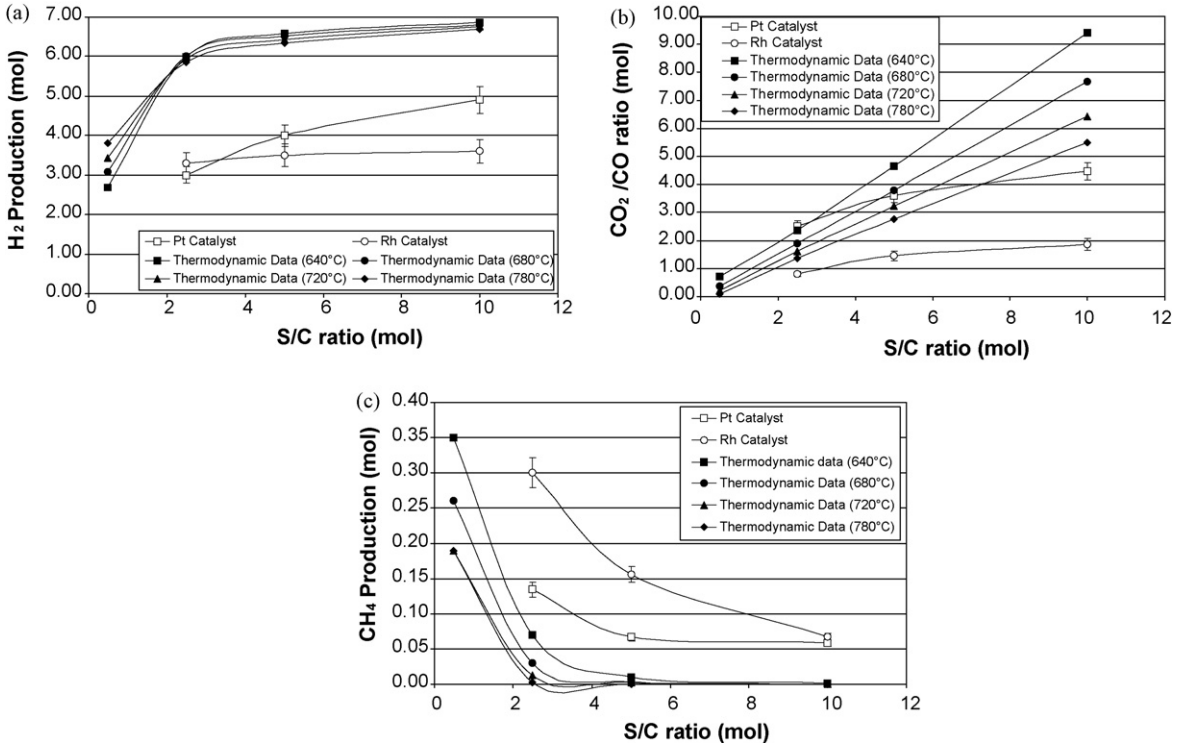


Fig. 3. $H_2$ production (a), $CO_2$/CO molar ratio (b) and $CH_4$ concentration (c) in function of the steam-to-carbon (S/C) molar ratios in the steam reforming of bio-oil over $Pt/Ce_{0.5}Zr_{0.5}O_2$ and $Rh/Ce_{0.5}Zr_{0.5}O_2$ on monolith catalysts at 780 °C. Comparison with thermodynamic data. Reaction conditions: 9 mL $h^{-1}$ $H_2O$ flow, 5, 2.5 and 1.2 mL $h^{-1}$ bio-oil flow, gas flow rate (Ar) = 100 mL $min^{-1}$. Data obtained from mass spectrometer analysis.

bio-oil sample used. The results are given in moles of hydrogen produced and $CO_2$/CO molar ratio per 100 g of processed bio-oil, as a function of the S/C ratio.

Increasing the S/C ratio from 2.5 to 10 over the Pt catalyst leads to an increase of $H_2$ production at both 700 °C (from 3 to 4 mole, Fig. 2a) and 780 °C (from 3 to 4.9 mole, Fig. 3a), following the thermodynamic trends. Over the Rh sample, this effect is less marked. The $CO_2$/CO molar ratio also increases by raising the S/C ratio from 2.5 to 10 (Figs. 2b and 3b), following the thermodynamic predictions. This tendency is respected at both reaction temperatures over the two catalysts tested. Nevertheless, the increase of $CO_2$/CO ratio is less important with the Rh catalyst. In the same time, the $CH_4$ production decreases when the S/C ratio increases (Fig. 2c). This tendency is more evident for the Rh catalyst than for Pt. Thus, at 700 °C the $CH_4$ production goes from 0.22 to 0.08 mole for the Pt sample (Fig. 2c), whereas with the Rh sample the $CH_4$ production is decreased by a factor of 10 (0.30 to 0.03 mole). These $CH_4$ concentrations are close to the values predicted by thermodynamic calculations, mainly at S/C = 10 (Fig. 2c). The same effect on $CH_4$ formation is observed at 780 °C (Fig. 3c).

Generally, the $H_2$ production and the $CO_2$/CO ratios obtained by steam reforming of crude bio-oil were lower than predicted by thermodynamic data, although they followed the expected trends when increasing the S/C molar ratio. Therefore, the catalysts appeared not active enough to reach the predicted equilibrium compositions, at the temperatures used. However, the calculated equilibrium compositions should be considered as only indicative, since they were calculated from a highly simplified reactants mixture compared to the very complex composition of the real bio-oil. Moreover, due to the high endothermicity of the steam reforming reaction, the effective temperature of the catalytic surface is probably lower than the one measured by the thermocouple located in the first third of the monolith axial length. This might explain that, in some cases (e.g. at low S/C ratio) the effective $CO_2$/CO ratio reported in Fig. 2b corresponds more to a thermodynamic value obtained at 640 °C rather than at the measured temperature of 700 °C.

The Pt-based catalyst was always more active than the Rh one and the products stream composition closer to that predicted by thermodynamics, mainly at high S/C molar ratios. Since the two metals are dispersed on the same ceria–zirconia support, these observations underline the higher WGS activity of Pt compared to Rh, as generally agreed in the literature [19].

In summary, the best catalytic activity was found over monolith-supported $Pt/Ce_{0.5}Zr_{0.5}O_2$ catalyst, both in terms of hydrogen production and selectivity. By working at 780 °C and S/C = 10, a hydrogen yield of 70% was obtained, while the methane concentration was lower than 1%. This result concerning the platinum activity in the steam reforming of bio-oil is in good agreement with the one reported in Ref. [16], describing steam reforming of bio-oils over Pt- and Rh-supported powder catalysts.

### *3.1.2. Catalyst evolution during steam reforming experiments*

As shown in previous studies [15,17], carbon deposition is a major issue during catalytic processing of bio-oils or its

Table 3
Effect of carbon deposition on the surface area of noble metals catalysts supported on monolith under steam reforming reaction conditions

| Catalyst | Conditions | $S_{Area}$ ($m^2/g$)[c] | Carbon (wt.%)[d] |
|---|---|---|---|
| $Pt/Ce_{0.5}Zr_{0.5}O_2$ on monolith | Fresh | 118 | 0.0 |
| | Coked[a] | 42 | 11.9 |
| | Regenerated[b] | 53 | 1.2 |
| $Rh/Ce_{0.5}Zr_{0.5}O_2$ $Pt/Ce_{0.5}Zr_{0.5}O_2$ on monolith | Fresh | 125 | 0.0 |
| | Coked[a] | 49 | 12.4 |
| | Regenerated[b] | 69.0 | 1.4 |

[a] Catalyst removed from the reactor after 1 h30 steam reforming under the reaction conditions: 5 mL/h of bio-oil, S/C molar ratio = 2.5, Temperature = 780 °C.
[b] Catalyst removed from the reactor after a regeneration under 20 vol.% $O_2$.
[c] Referred to the washcoat only (not including the cordierite mass).
[d] Determined by chemical analysis.

components. A significant amount of coke was found to accumulate on both catalysts during the steam reforming reaction (Table 3). The amount of deposited coke (≈12 wt.% after 1 h30 time on stream) appeared similar for both catalysts. In the same time, both catalysts showed a ca. 60% decrease of their specific surface areas. Carbon removal under oxygen flow (20 vol.% in argon) only partially recovered the specific surface area lost during the steam reforming. Therefore, in addition to coke deposition, the steam reforming conditions also led to a substantial sintering of the ceria–zirconia washcoat for both $Pt/Ce_{0.5}Zr_{0.5}O_2$ and $Rh/Ce_{0.5}Zr_{0.5}O_2$ monolithic catalysts. However, both phenomena apparently did not result in catalyst deactivation over the tested period, as expected from systems essentially controlled by thermodynamics, at least for the overall conversion.

### 3.2. Sequential cracking/reforming of bio-oil over Pt and Rh monolithic catalysts

Platinum and rhodium catalysts deposited on cordierite monolith were also tested in the sequential cracking of crude bio-oil. The idea is to alternate a cracking reaction step, in which the bio-oil is transformed into gaseous products ($H_2$, $CH_4$, CO, $CO_2$) and solid carbon deposited on the catalyst, with a regeneration step where the coke is removed by combustion. Taking into account that no steam is added in the feed, this configuration can be considered as an attempt to improve the energetic efficiency of the whole process.

The catalytic performance of a $Pt/Ce_{0.5}Zr_{0.5}O_2$ catalyst deposited on cordierite monolith for the sequential cracking of bio-oils is shown in Fig. 4, where only seven consecutive cracking/regeneration sequences are depicted for a better readability. During the cracking steps, the bio-oil is entirely converted into $H_2$, CO, $CO_2$, $CH_4$ and C deposited on the catalyst. The amounts of other products observed during cracking were always negligible (<0.5%). In addition, water was permanently present in the reactor, both as reactant (the crude bio-oil contains 28.8 wt.% $H_2O$) and as product (resulting from the WGS equilibrium). An enlargement of one cracking/regeneration sequence obtained with the stabilized Pt catalyst (after at least five cracking/regeneration sequences) is presented in Fig. 5. The average gas products composition obtained by GC analysis (performed at periodic time intervals at the end of each cracking step) are given at the end of Table 2 for both $Pt/Ce_{0.5}Zr_{0.5}O_2$ and $Rh/Ce_{0.5}Zr_{0.5}O_2$ monolithic catalysts. These values were calculated on dry basis taking into account only the four main gaseous products ($H_2$, $CH_4$, CO and $CO_2$).

In the case of monolithic $Pt/Ce_{0.5}Zr_{0.5}O_2$, the bio-oil cracking step occurred with a high selectivity to $H_2$ and CO (49 and 30 vol.%, respectively, Table 2) meanwhile, the methane production reached 7 vol.%. The continuous monitor-

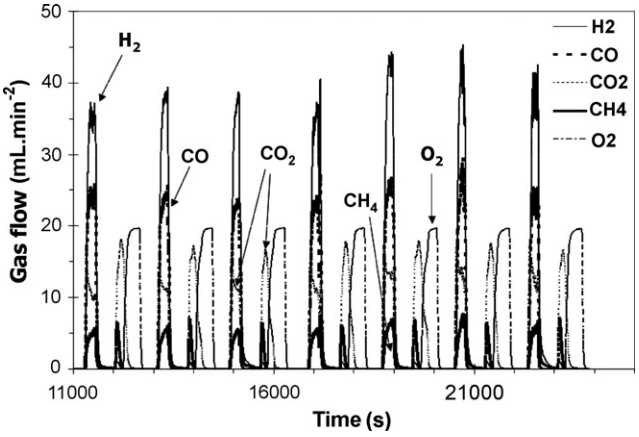


Fig. 4. Sequential cracking of bio-oil over $Pt/Ce_{0.5}Zr_{0.5}O_2$ on monolith (seven sequences). Reaction conditions: 700 °C, 5 mL $h^{-1}$ bio-oil flow, gas flow rate (Ar) = 100 mL $min^{-1}$; 5 min of cracking, 10 min of regeneration. Products gas flows (mL $min^{-1}$) as monitored by mass spectrometry.

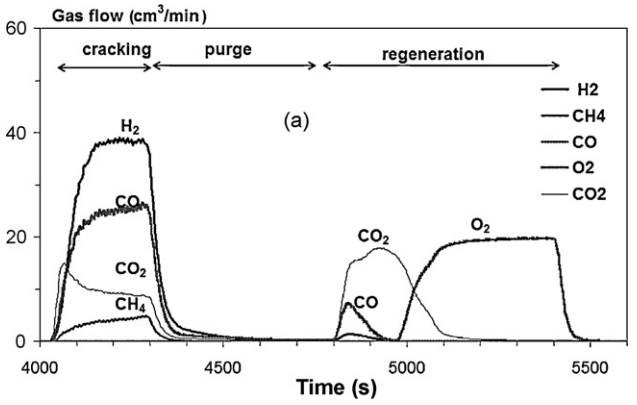


Fig. 5. Gaseous products composition (on dry basis) obtained during one cracking/regeneration sequence over monolithic $Pt/Ce_{0.5}Zr_{0.5}O_2$ as function of time. Reaction conditions: 700 °C, 5 mL $h^{-1}$ bio-oil flow, gas flow rate (Ar) = 100 mL $min^{-1}$.

ing by MS (Fig. 5) showed that $H_2$ production started rapidly when the cracking reaction begun, reaching a maximum of ~38 mL/min. Hydrogen was then produced continuously at constant level all along the cracking step. A high amount of CO was also formed, while the $CH_4$ production was always lower than 5 mL/min. In addition, coke is also produced and stored on the catalyst during the cracking process (≈35 mg for one sequence).

The $Rh/Ce_{0.5}Zr_{0.5}O_2$ monolithic catalyst behaved similarly in the sequential cracking of bio-oil (Table 2). The $H_2$ concentration was 52% and it remained constant ($H_2$ flow ~40 mL/min) even after a long-term experiment with more than 30 cracking/regeneration sequences. After 12 sequences, $H_2$ production and product gas composition were similar to those achieved by the Pt-based catalyst.

In general, the $H_2$ production decreased slightly along the sequences, and the deactivation was more evident with Pt than with Rh-based catalyst. This phenomenon is related to a sintering of the ceria–zirconia support revealed by TEM analysis (micrographs not shown), in agreement with the specific surface area decrease observed after steam reforming experiments (Table 3).

Sequential cracking experiments carried out in the absence of catalyst revealed that the bio-oil is fully converted by gas phase thermal reactions, $H_2$, CO, $CO_2$ and $CH_4$ being the main products, with however a much lower hydrogen productivity of ca. 10 mmol $H_2/g_{bio\text{-}oil}$ (Table 2). Moreover, the $H_2$ formation was not stable and decreased along the cracking steps. The regeneration revealed a strong $CO_2$ formation, while no CO was detected. However, the deposited coke was not fully burnt during the regeneration steps.

Comparison of the quantitative results obtained in the presence and in the absence of catalysts (Table 2) showed that the use of catalysts deposited on monoliths allowed a constant production of hydrogen of ca. 18 mmol $H_2/g_{bio\text{-}oil}$ all along the cracking step as well as a high catalytic stability. The complete conversion of bio-oil in the absence of catalyst revealed the existence of both thermal and catalytic processes. However, the catalyst played a major role in ensuring a continuous $H_2$ production, improving the conversion of bio-oil into gaseous compounds and reducing the formation of undesired compounds. The $CH_4$ concentration strongly decreased in the presence of catalyst (from 11% to 6%), which is likely related to the capacity of the catalyst to steam reform methane with the water contained in the bio-oil. The water content of bio-oil around 29 wt.% corresponds to a steam-to-carbon ratio of 0.5 in the sequential cracking reaction.

The hydrogen productivities achieved during the sequential process (Table 2) are actually in good agreement with the theoretical $H_2$ amount that can be produced considering a reforming process at S/C ratio = 0.5 (≈20 mL $H_2$/min). This is illustrated in Fig. 2, showing that the hydrogen production and the $CO_2$/CO ratios at S/C = 0.5 are close to the values predicted by the thermodynamic equilibrium, for both Pt and Rh catalysts. The $CO_2$/CO ratio slightly higher than the calculated value could be attributed to thermal effects (lower effective catalyst temperature than measured) as already proposed for the steam reforming data. However, the oxygen storage capacity of ceria–zirconia support [19] could also be involved in the sequential process. At each regeneration step, the ceria–zirconia support is reoxidized, and this mobile lattice oxygen is available in the next cracking step to oxidize part of the depositing carbon into $CO_2$. Clearly, the differences in catalytic performances between Pt and Rh catalysts in the steam reforming experiments at S/C ≥ 2.5 are minimized under cracking/reforming conditions. This is probably related to the lower impact of the WGS reaction at S/C = 0.5, for which the Pt catalyst is more active than Rh.

### 3.3. Comparison of sequential cracking and steam reforming reactions

The sequential cracking allows to directly process bio-oils without water addition, and therefore requires lower energy consumption (vaporization step not necessary). An estimation of heat balance during cracking (endothermic) and regeneration (exothermic), showed that the process could run auto-thermally, provided the heat of carbon combustion is efficiently recovered [18]. By using two (or more) parallel reactors, it is possible to ensure a continuous $H_2$ production for a molten carbonate fuel cell, which can accommodate large amounts of CO. Pt and Rh catalysts deposited on monoliths achieve hydrogen productivities of 17 and 18 mmol $H_2/g_{bio\text{-}oil}$, respectively. These $H_2$ productivities are not so far from those obtained by steam reforming at S/C = 2.5 over both catalysts, when similar temperature and bio-oil feed are used (21 mmol $H_2/g_{bio\text{-}oil}$ with Pt and Rh catalysts). In addition, the periodical catalyst regeneration allows a good control of coke combustion and therefore the long-term catalysts deactivation could be avoided. In addition, this separate step of coke combustion could allow a partial $CO_2$ sequestration. Recently, by combining a Ni-based methane steam reforming catalyst with a $CO_2$-sorbant in two reactors working alternately, Li et al. [20] showed that $CO_2$ can be efficiently separated, leading to high-purity hydrogen coupled to $CO_2$ sequestration. Nevertheless, a further improvement in sequential cracking process is necessary to decrease CO (<18%) and $CH_4$ (<5%) to levels corresponding to the MCFC [21] required specifications.

On the opposite, the $H_2$ productivity by steam reforming can be enhanced up to ~49 mmol $H_2/g_{bio\text{-}oil}$ at 780 °C and S/C = 10 over monolithic $Pt/Ce_{0.5}Zr_{0.5}O_2$ catalyst. The steam reforming process also leads to lower CO amounts and practically no $CH_4$ in the gaseous products stream, this being clearly an advantage.

## 4. Conclusions

Hydrogen production from biomass-derived oil via both steam reforming and sequential cracking processes was efficiently performed over platinum- and rhodium-based catalysts supported on cordierite monolith.

Comparison of $Pt/Ce_{0.5}Zr_{0.5}O_2$ and $Rh/Ce_{0.5}Zr_{0.5}O_2$ monolithic catalysts under similar reaction conditions reveals that the Pt catalyst always achieves higher $H_2$ productivities than Rh in steam reforming of bio-oil. This performance is attributed to the

Pt ability to promote the WGS reaction, which is enhanced at high steam-to-carbon ratio.

In the case of sequential cracking, both Pt and Rh catalysts allow a constant and continuous production of hydrogen all along the cracking step, with however a lower productivity than that obtained by steam reforming. The catalytic behaviour of both catalysts is very similar. The noble metal ensures an efficient control of carbon deposition and removal, the coke formed during cracking being fully burnt during the regeneration step. The complete conversion of biomass-derived oil even in the absence of catalyst reveals the existence of both thermal and catalytic processes. The catalyst plays a major role in enhancing the hydrogen yield and reducing the formation of undesired compounds. Thus, methane and CO concentrations are decreased in presence of catalyst to reach the appropriate levels for fuel cell specifications.

Thus, by adequately adjusting the reaction conditions, both steam reforming and sequential cracking/reforming processes could be used as an alternative hydrogen source for fuel cells. An integrated process would involve the direct processing of bio-oil connected to a fuel cell capable to support fuel flexibility, such as a MCFC or a SOFC [21,22]. An overall efficiency of ca. 80% could be reached by heat co-generation, with less acoustic and pollution nuisance when compared to combustion technologies. Moreover, bio-oils can be transported and stored, which suppresses the need of placing the electrical power source in the vicinity of the biomass collection center. This approach could be applied in small-scale decentralized systems or in residential areas, where severe environmental regulations for gas emissions are imposed.

## Acknowledgments

This work was funded by the European Commission (5th FP: ''Bioelectricity'', ENK5-CT-2002-00634). We gratefully acknowledge the assistance of Johnson Matthey (UK), and University of Twente (Netherland), and we thank the Bioelectricity partners: Ansaldo and Enea (Italy), Queen's University Belfast (Ireland) and University of Patras (Greece).

## References

[1] M. Marquevich, F. Medina, D. Montané, Catal. Commun. 2 (2001) 119.
[2] R.R. Davda, J.A. Dumesic, Chem. Commun. (2004) 36.
[3] K.M.F. Kazi, P. Jollez, E. Chornet, Biomass Bioenergy 15 (2) (1998) 125.
[4] S. Rapagnà, N. Jand, P.U. Foscolo, Int. J. Hydrogen Energy 23 (1998) 551.
[5] A. Demirbas, Energy Sources 24 (2002) 59.
[6] D. Wang, S. Czernik, E. Chornet, Energy Fuels 12 (1998) 19.
[7] A.V. Bridgwater, S. Czernik, J. Piskorz, in: A.V. Bridgwater (Ed.), Fast Pyrolysis of Biomass: A Handbook, vol. 2, CPL Press, Newbury, UK, 2002, pp. 1–22.
[8] A. Oasmaa, D. Meier, in: A.V. Bridgwater (Ed.), Fast Pyrolysis of Biomass: A Handbook, vol. 2, CPL Press, Newbury, UK, 2002, pp. 41–58.
[9] J.R. Galdámez, L. García, R. Bilbao, Energy Fuels 19 (2005) 1133.
[10] S. Czernik, R.J. French, K.A. Magrini-Bair, E. Chornet, Energy Fuels 18 (2004) 1738.
[11] D. Wang, S. Czernik, D. Montané, M. Mann, E. Chornet, Ind. Eng. Chem. Res. 36 (1997) 1507.
[12] D. Wang, D. Montané, E. Chornet, Appl. Catal.: Gen. 143 (1996) 245.
[13] K. Polychronopoulou, C.N. Costa, A.M. Efstathiou, Appl. Catal.: Gen. 272 (2004) 37.
[14] K. Takanabe, K. Aika, K. Seshan, L. Lefferts, J. Catal. 227 (2004) 101.
[15] L. García, R. French, S. Czernik, E. Chornet, Appl. Catal. A: Gen. 201 (2000) 225.
[16] C. Rioche, S. Kulkarni, F.C. Meunier, J.P. Breen, R. Burch, Appl. Catal. B: Environ. 61 (2005) 130.
[17] T. Davidian, N. Guilhaume, E.E. Iojoiu, H. Provendier, C. Mirodatos, Appl. Catal. B: Environ. 73 (2007) 116.
[18] E.E. Iojoiu, M.E. Domine, T. Davidian, N. Guilhaume, C. Mirodatos, Appl. Catal. A: Gen. 323 (2007) 147.
[19] P. Panagiotopoulou, D.I. Kondarides, Catal. Today 112 (2006) 49.
[20] Z. Li, N. Cai, J. Yang, Ind. Eng. Chem. Res. 45 (2006) 8788.
[21] C. Iaquaniello, A. Mangiapane, Int. J. Hydrogen Energy 31 (2006) 399.
[22] T. Kivisari, P. Bjoernbom, C. Sylwan, J. Power Sources 104 (2002) 115.